Generation of Range-based Trajectories Using a Unicycle

Twinkle Tripathy and Ritick Gupta

***Abstract*— The paper focuses on the generation of planar trajectories using an autonomous agent modelled as a unicycle. The agent can be controlled using its linear and angular speeds. It is assumed that only range information is available to the agent with respect to a stationary point, known as the target. The latter could is representative of any beacon, a building of interest or a landmark in real world scenarios. Both of the speeds are designed as continuous functions of range with the linear speed constrained to be positive. We present a complete characterisation of agent trajectories in the given framework which shows that the trajectories can remain bounded or become unbounded depending on both the control inputs and the initial conditions. We also present the conditions necessary to generate each kind of the above mentioned trajectories. Finally, numerical simulation have been presented to elucidate the results.**

I. Introduction

Autonomous agents like fixed wing aircrafts, ground vehicles, submarines, *etc.* are widely used to serve numerous applications as cleaning systems, lawn mowers, surveillance systems, agricultural tools, *etc.*. Hence, the trajectories of autonomous agents are to be suitably generated in accordance. These desired trajectories can also be generated by shaping the trajectories as mathematical curves [1], [2]. This approach has drawn the interest of the research community for over several decades now. They have been used to address problems like coverage [3], target capture [4], [5] and boundary surveillance [6]. The inspiration stems from the occurrence of such curves in nature like intricate paths of astronomical objects, pursuit evasion motions of a prey and predator, combat motions of dragon flies and so on.

In this work, we focus on the generation of trajectories of desired bounds and shape, which are aesthetically appealing and can also serve real world applications like (differentiated) surveillance and coverage. Such trajectories can be generated with a single or a team of autonomous agents. In general, the latter can be achieved by suitably controlling the spacial arrangements of the agents, also referred to as the formation control problem [7]. Local interactions in a cooperative set-up can lead to desired inter-agent global formations. There are several works in the literature wherein agents get into stationary formations while moving in circles or polygons [8], [9]. Formations can be dynamic with rectilinear, polygonal, etc. motions of the agents while they maintain relative spatial arrangements with respect to each other ([10], [11]). Yet another way to achieve desired intricate motions is to employ path following strategies for single or multiple autonomous agents [12], [13].

The results presented in this paper are along the same lines as those in [14], [15], [16], [17] which focus on the generation of intricate periodic and bounded trajectories. These works mostly explore the generation of exquisite hypo-trochoidal trajectories. Tsiotras *et al.* employ a state-feedback based guidance law to achieve consensus among the agents [14]. Using a constant bearing strategy, Galloway *et al.* generate perioidic orbits pertaining to the trajectories of agents in cyclic pursuit. Using another variant of the cyclic pursuit strategy, proposed by Juang in [16], intricate trajectories result through local interactions. In one of our earlier works, we analysed the trajectories of a unicycle agent when only range information is available to it. It revealed a plethora of intricate trajectories beyond the hypotrochoids, which were categorised into bounded (and periodic) and unbounded ones.

All of the works discussed in the preceding paragraph consider an autonomous agent modelled as a unicycle moving at a constant speed. In contrast to it, in this work, we extend the analysis to allow the agent to have a variable speed. The autonomous agent is assumed to have range information with to respect to a stationary target point which could denote a beacon, landmark, *etc*. in real world applications. The linear and angular speeds are designed as continuous functions of the range. Analysis of the trajectories leads to a wider set of trajectories as compared to those achieved in our previous works [17]. We also present a complete characterisation of the trajectories in terms of the given inputs and initial conditions. The conditions necessary to achieve desired bounds are also presented. The rest of the paper is organised as follows: Sec. II gives a mathematical formulation of the work. In the given framework, the analysis of the trajectories are presented in Sec. III. Simulation results are presented in Sec. IV. Sec. V Conclusions along with some insights into the future work are presented.

II. Problem Formulation

The paper analyses the trajectories of an autonomous agent when only range measurements are available. The agent, A, has kinematics of a point-mass unicycle system, given by,

$$\dot{x} = v\cos\alpha, \tag{1a}$$

$$\dot{y} = v\sin\alpha, \tag{1b}$$

$$\dot{\alpha} = u \tag{1c}$$

Twinkle Tripathy is an Assistant Professor with Department of Electrical Engineering, Indian Institute of Technology, Kanpur - 208016, India, ttripathy@iitk.ac.in.

Ritick Gupta is an undergraduate student with Department of Electrical Engineering, Indian Institute of Technology, Kanpur - 208016, India, ritickg20@iitk.ac.in.

where (x, y, α) is the pose of the unicycle agent, v and u are two control inputs governing the linear and angular speeds of the agent.

In real world scenarios, the use of sensors are subject to factors like available resources, constrained sensing radii, *etc*. With this in mind, we consider the problem where only range information is available where range refers to the distance between the agent and a pre-defined target point, T. In real world scenarios, the target point can be a building of interest, a landmark or a beacon with respect to which the trajectories of the agent are analysed. The planar geometry between the agent and the target is shown in Fig. 1. As shown in the figure, r is the Euclidean distance between the agent and the target and θ is the line-of-sight (LOS) angle between them. The parameter r is referred to as the range.

Unlike our previous works, which focused on the trajectories generated by a unicycle agent moving with a constant linear speed, here we control both linear and angular speeds, v and u, respectively. To begin with, a generic form of the inputs are considered,

$$v = v(r) \geqslant 0 \tag{2a}$$

$$u = u(r) \tag{2b}$$

where $u(r)$ can be any continuous functions of the range r, while $v(r)$ is assumed to be a positive continuous function of r. The latter implies that the agent can move only in the forward direction. Our objective is to analyse and characterise the trajectories generated by the agent when only range information is available.

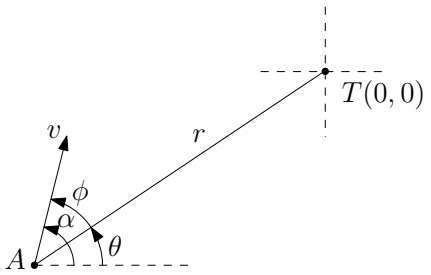

Fig. 1: Planar geometry between the agent and the target

III. Analysis of Trajectories

For ease of analysis, we re-write the kinematics of the agent, mentioned in (1), in a polar coordinate frame of reference as $\dot{r} = -v(r)\cos(\alpha - \theta)$ and $\dot{\theta} = -\frac{v}{r}\sin(\alpha - \theta)$. Now, we introduce a parameter ϕ defined as,

$$\phi = \alpha - \theta \tag{3}$$

The simplified kinematics is then given by,

$$\dot{r} = -v(r)\cos\phi, \tag{4a}$$

$$\dot{\theta} = -\frac{v(r)}{r}\sin\phi \tag{4b}$$

and,

$$\dot{\phi} = u(r) + \frac{v(r)}{r}\sin\phi. \tag{5}$$

We observe that eqns. (4a) and (5) depend only on r and ϕ. This implies that the evolution of the parameters r, θ, α and ϕ is governed by these parameters as elaborated through the following result.

Lemma 1: The trajectories of an autonomous agent with unicycle kinematics (1) and control inputs (2) evolve on the manifold defined by,

$$\mathcal{M}(r, \phi) := \{(r, \phi) : f(r) + r\sin\phi - K = 0\} \tag{6}$$

where $f(r)$ is the antiderivative of $ru(r)/v(r)$ and $K = f|_{t=0} + v\sin\phi|_{t=0}$ depends on the initial conditions.

Proof: Combining eqns. (4a) and (5), we get $(ru(r) + v(r)\sin\phi)dr + rv(r)\cos\phi\ d\phi = 0$. This differential equation is not exact as $\partial(ru(r) + v(r)\sin\phi)/\partial\phi \neq \partial(rv(r)\cos\phi)/\partial r$. In order to make it exact, we use the integrating factor $\frac{1}{v(r)}$. Multiplying the differential equation with the integrating factor, we get,

$$\left(\frac{ru(r)}{v(r)} + \sin\phi\right)dr + r\cos\phi\ d\phi = 0 \tag{7}$$

Integrating this modified differential equation gives (6). ■

For time $t \geqslant 0$, the trajectory of the unicycle always satisfies (6). Several important factors pertaining to the trajectory like boundedness, shape of the trajectory, *etc*. can be determined using this equation. Next, we explore some properties of the trajectories of the autonomous agent in the given framework.

A. The generating functions

Before proceeding with the analysis, we introduce a variable $g(r) : \mathbb{R} \to \mathbb{R}$ defined as $g(r) = f(r) - K$ where $f(r)$ is given by (6). Then, it is obvious that,

$$g(r) = -r\sin\phi \tag{8}$$

We know that from Lemma 1 that $f(r)$ is the antiderivative of $ru(r)/v(r)$. Since $g(r) = f(r) - K$, taking a derivative, we get,

$$u(r) = \frac{1}{r}\frac{dg(r)}{dr}v(r). \tag{9}$$

Eq. (9) gives us a way to design $u(r)$ and $v(r)$ for a given generating function $g(r)$. Given any inputs $v(r)$ and $u(r)$ and initial conditions, we can find $g(r)$ uniquely. For example, for $u(r) = 2r - 6$, $v(r) = r$ and initial conditions $(r_0, \phi_0) = (2, 3\pi/2)$, we get $g_2(r) = r^2 - 6r + 10$ which is shown in Fig. 2.

Remark 2: We would like to highlight that fact that, unlike the results presented in our previous works [17], this equation does not explicitly dependent on speed $v(r)$. Owing to this, the analysis which follows reveals new kinds of trajectories which aren't possible to get generated for a unicycle moving with constant speed.

Next, we explore some scenarios which lead to stationary points in the trajectory with respect to all or some of the parameters.

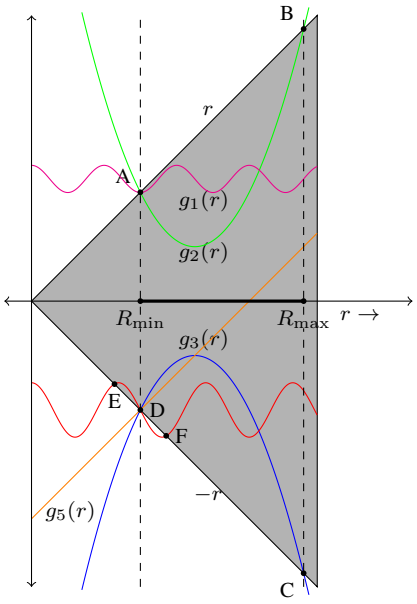

Fig. 2: Generating functions

Lemma 3: Given any $v(r)$, $u(r)$ and initial conditions, the trajectory of an autonomous agent with kinematics (1) and control inputs (2), converges to a single point $(\bar{x}, \bar{y})$ if,

$$u(\bar{r}) = 0, \tag{10a}$$
$$v(\bar{r}) = 0 \tag{10b}$$

and the trajectory evolves such that $r(t) = \bar{r}$ for some $t \geqslant 0$ where $\bar{r} = (\bar{x}^2 + \bar{y}^2)^{0.5}$.

Proof: It follows from (4a) that $\dot{r}|_{r=\bar{r}} = 0$ for (10). This implies that $\bar{r}$ is a point of extremum. In order to determine its nature, we evaluate the second derivative by differentiating (4a) to get,

$$\ddot{r}|_{r=\bar{r}} = v(r)\sin\phi\ \dot{\phi} - \dot{v}(r)\cos\phi\ \dot{r} \tag{11}$$

Substituting (10) in (5) gives $\dot{\phi}|_{r=\bar{r}} = u(\bar{r}) + \bar{v}\sin\phi/\bar{r} = 0$. Hence, $\ddot{r} = 0$. It can be shown in a similar manner that all the higher derivatives of r also go to zero. Hence, once the trajectory reaches a point in the $\mathbb{R}^2$ plane at which $r = \bar{r}$ and (10), $r = \bar{r}$ is maintained from that point of time onwards. This ensures that (10) also holds implying that the speed of the agent remains zero. Therefore, the trajectory converges to this particular point in $\mathbb{R}^2$. ■

An interesting point to note in Lemma 3 is that the nature of $v(r)$ is immaterial as long as (10) holds. A similar behaviour occurs in the following scenario.

Lemma 4: Given any $u(r)$, $v(r)$ and initial conditions, the trajectory of an autonomous agent with kinematics (1) and control inputs (2), converges to a $\bar{r} > 0$ if,

$$g(\bar{r}) = \pm\bar{r} \tag{12}$$
$$\frac{dg(r)}{dr}|_{r=\bar{r}} = \pm 1 \tag{13}$$

and the trajectory evolves such that $r(t) = \bar{r}$ for some $t \geqslant 0$.

Proof: It follows from (4a) that $\dot{r}|_{r=\bar{r}} = 0$ for (10). This implies that $\bar{r}$ is a stationary point. The value of $\bar{\phi}$ is determined using (5) and is given by,

$$\dot{\phi}|_{r=\bar{r}} = u(\bar{r}) + \sin\phi/\bar{r}. \tag{14}$$

From (8), we get $\sin\phi = 3\pi/2$ for $g(r) = r$ and $\pi/2$ for $g(r) = -r$. Then, using (9) and substituting (12) and (13), we get $u(\bar{r}) = v(\bar{r})(\frac{1}{r}\frac{dg(r)}{dr} + \sin\phi/\bar{r}) = 0$. This implies $\ddot{r} = 0$. It can observed that we have now reached the same conditions as those in Lemma 3. Hence, the rest of the proof also follows in the same manner as that of Lemma 3. ■

Unlike Lemma 3 in which the trajectory converges to a point, in this case r becomes constant. These are some simple behaviours of the unicycle arising in specific scenarios. In general, however, both $u(r)$ and $v(r)$ shape the trajectories of the agent such that intricate trajectories can be generated as presented in Section IV. Our objective is to now find the relation between the trajectories and the control inputs. We start by analysing the characteristics of the generating functions. Given inputs $v(r)$ an $u(r)$ and initial conditions, (6) can hold only when $-r \leqslant g(r) \leqslant r$ as $\sin\phi \in [-1, 1]$. This region is shaded in gray in Fig. 2. Correspondingly, the values of r which satisfy this condition for a given $g(r)$ form the set of feasible values of r. Within this set, a subset of r values can satisfy (6). Some points in the latter set have special significance.

(i) Entry point $r = r_{en}$: It is the point at which $g(r)$ enters the region in which $-r \leqslant g(r) \leqslant r$.
(ii) Tangential point $r = r_t$: It is the point at which $g(r)$ is tangent to the line r or $-r$.
(iii) Exit point $r = r_{ex}$: It is the point at which $g(r)$ exits the region in which $-r \leqslant g(r) \leqslant r$.

These points are of significance as explained below.

Lemma 5: Consider an agent with unicycle kinematics (1) and control inputs $u(r)$ and $v(r)$ as given in (2). In the region where the generating function (8) satisfies $g(r) \in [-vr, vr]$, if r becomes equal to $\bar{r} \in \{r_{en}, r_t, r_{ex}\}$, then the following behaviours arise:

- $\bar{r} = r_{en}$: The value of r is lower bounded by the entry point such that $\min(r) = r_{en}$.
- $\bar{r} = r_t$: The value of r remains equal to r_t thereafter $r = r_t$.
- $\bar{r} = r_{ex}$: The value of r is upper bounded by the exit point such that $\max(r) = r_{ex}$.

The proof relies on the fact that $\dot{r} = 0$ only for $\phi = \pi/2$ or $3\pi/2$ i.e. on the lines $\pm r$. So, the intersection point of $g(r)$ with these lines must correspond to the extrema of r. The nature of the extrema are given by analysing the second derivative of r (which is positive for r_{en} and negative for r_{ex}). At a tangential point, all the higher derivatives of r go to zero, making it a stationary point. Hence, this lemma is useful in characterising the trajectories of the unicycle. For a detailed proof, the readers are directed to [17] for the proof of the result.

In general, a generating function may not have always have an exit and/or tangential point, while it always has an

entry point. For example, the generating function $g_1(r) = 0.25\cos(1.5\pi r) + 2.245$ only has an entry point $r_{en} = 2$. This implies that the trajectory that gets generating is strictly lower bounded by the entry point such that $\min(r) = 2$. Hence, the trajectories of the agent depends on the points r_{en}, r_t and r_{ex} which, in turn, depend on the generating functions. However, several questions still remain. For example, the generating function $g_1(r)$ does not have an exit point. So the question arises that does the lack of an exit imply that the trajectory can not be upper bounded? We answer this question through the following result.

Theorem 6: For an autonomous agent with unicycle kinematics (1), consider the control inputs (2) and initial conditions x_0, y_0 and α_0. Depending on the generating function $g(r)$ defined in (8), the trajectory of the agent can be categorised as,

(i) bounded and periodic if $g(r)$ has an r_{en} and an r_{ex} with $r_t, \bar{r} \notin [r_{en}, r_{ex}]$ and $r_0 \in [r_{en}, r_{ex}]$,

(ii) unbounded when
- $r_0 \in [r_{en}, \infty]$ with $r_{ex}, \bar{r} \notin [r_{en}, \infty]$,
- $r_0, r_t \in [r_{en}, \infty]$ with $r_{ex}, \bar{r} \notin [r_{en}, \infty]$ with $\phi_0 \in (\pi/2, 3\pi/2)$ for $r_0 > r_t$,

(iii) converges to the point $r = \bar{r}$ if $g(\bar{r}) \in [-vr, vr]$ and the initial conditions satisfy,
- $r_0, \bar{r} \in [r_{en}, r_{ex}]$ such that $r_t \notin [r_{en}, \bar{r}]$,
- $r_0, \bar{r} \in [r_{en}, \infty]$ such that $r_{ex}, r_t \notin [r_{en}, \infty]$ with $\phi_0 \in (-\pi/2, \pi/2)$ for $r_0 > \bar{r}$,
- $r_0 \in (r_t, \bar{r}]$, $r_{en}, r_{ex} \notin (r_t, \bar{r})$ and $\phi_0 \in (\pi/2, 3\pi/2)$ or $r_0 \in (\bar{r}, r_t)$, $r_{en}, r_{ex} \notin (\bar{r}, r_t]$ and $\phi_0 \in (-\pi/2, \pi/2)$ or $r_0 = \bar{r}$,

(iv) circular when $g(r)$ has an r_t such that,
- $r_0, r_t \in [r_{en}, r_{ex}]$ such that $\bar{r} \notin [r_e n, r_{ex}]$,
- $r_0, r_t \in [r_{en}, \infty]$ with $r_{ex}, \notin [r_{en}, \infty]$ with $\phi_0 \in (-\pi/2, \pi/2)$ for $r_0 > r_t$,

where r_{ex} (if it exists,) is the nearest exit point larger than r_{en} such that $-r \leq g(r) \leq r$ for every $r \in [r_{en}, r_{ex}]$ and $\bar{r}$ satisfies (10).

Proof: We begin with condition (i) in which $g(r)$ has an r_{en} and r_{ex} with the latter being the nearest exit point larger than r_{en}. This implies that in the region $[r_{en}, r_{ex}]$, there are no other extrema and also, $-r \leq g(r) \leq r$. Then, Lemma 5 says that r_{en} lower bounds the instantaneous values of r, while r_{ex} upper bounds. Moreover, due to the lack of other extrema in the region, r varies monotonically between r_{en} and r_{ex}. Thus, if $r_0 \in [r_{en}, r_{ex}]$, then $r(t) \in [r_{en}, r_{ex}]$ for every $t \geqslant 0$. Moreover, if we start at $r_0 = r_{en}$, then it can be shown easily by studying $\dot{r}$ and $\ddot{r}$ in $[r_{en}, r_{ex}]$ that we return to r_{en} in some finite time $T > 0$. Since we follow the same kinematics (1) again from $r = r_{en}$, we will return to r_{en} in the same time T, implying periodicity in r.

As we move to condition (ii), we consider generating function which do not have exit points. They may or may not have tangential points. If there are no tangential points, following the reasoning of the previous case, the trajectory increases monotonically from r_{en} causing the trajectory to be unbounded. In case there is a tangential point r_t, the initial condition must be such that we avoid it. If $\phi_0 \in (\pi/2, 3\pi/2)$ for any $r_0 > r_t$, then $\dot{r} > 0$. Owing to the monotonicity of r, the trajectory then becomes unbounded.

Sometimes the trajectory can converge to a single point as discussed in (iii). This can only happen when there is a stationary point $\bar{r}$ satisfying (10). The proof follows from Lemma 3. However, the trajectory must evolve such that r reaches $\bar{r}$. Using the proofs presented for conditions (i) and (ii), it can be shown that $r = \bar{r}$ is ensured if the initial conditions satisfy the conditions given in condition (iii).

By definition, a tangential point r_t occurs when $g(r_t) = \pm r_t$ and $\frac{dg(r)}{dr} = \pm 1$. In this case, we know from Lemma 4 that the instantaneous values of r converge to r_t if $r = r_t$ is reached. Then, the trajectory of the agent becomes circular with respect to the target point. However, this requires that the trajectory should reach the state $r = r_t$. It can be easily shown that this is guaranteed by following the conditions in (iv).

Hence, proved. ■

Theorem 6 shows the significance of generating functions in the determination of the nature of the trajectories. For example, the generating function $g_3(r) = -r^2 + 6r - 10$ has $r_{en} = 2$ and $r_{ex} = 5$. According to Theorem 6, the trajectory will be bounded with $\max(r) = 5$ and $\min(r) = 2$. However, the generating function $g_1(r) = 2.245 + 0.25\cos(1.5\pi r)$ only has an entry point $r_{en} = 2$, but no exit point. Hence, the trajectory will eventually become unbounded. Note that if these generating functions had tangential points or points satisfying (10), then such trajectories aren't guaranteed, irrespective of the control inputs $u(r)$ and $v(r)$. Nonetheless, Theorem 6 gives us a methodology to design control inputs $u(r)$ and $v(r)$ as elaborated below.

B. Designing the control inputs $u(r)$ and $v(r)$

In this subsection, we explore approaches to design $u(r)$ and $v(r)$ to achieve trajectories of our interest.

- *Trajectories with desired radial bounds*: In order to achieve a bounded trajectory of inner and outer radii $R_{\min}$ and $R_{\max}$, Theorem 6 says that the corresponding generating function $g(r)$ should be designed so that: $r_{en} = \min(r(t)) = R_{\min}$ and $r_{ex} = \max(r(t)) = R_{\max}$. Moreover, $-r \leqslant g(r) \leqslant r$ must hold $\forall r \in [R_{\min}, R_{\max}]$. It follows that the initial value of r_0 must lie in $[R_{\min}, R_{\max}]$, the corresponding ϕ_0 can be calculated using (8).
- *Trajectories with desired shape:* Since $g(r) = f(r) - K = \int ru(r)dr/v(r) - K$, it follows that the same generating function can be achieved for multiple combinations of the pair $(u(r), v(r))$. Given a $g(r)$, varying the $(u(r), v(r))$ pair results in trajectories of the same bounds, but different shapes. For example, given two continuous functions $p(r)$ and $q(r)$, the pairs $(p(r), q(r))$ and $(p(r)/q(r), 1)$ have the same generating function causing the bounds of the corresponding trajectories to be the same. However, since $\dot{\alpha} = u(r)$ is different in both the cases, their shapes are different.

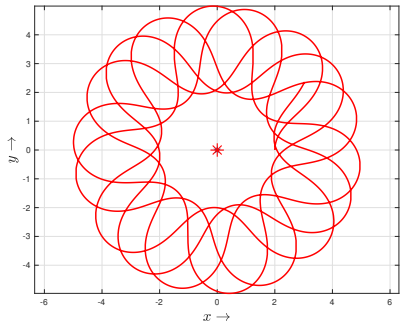

(a) Agent trajectory

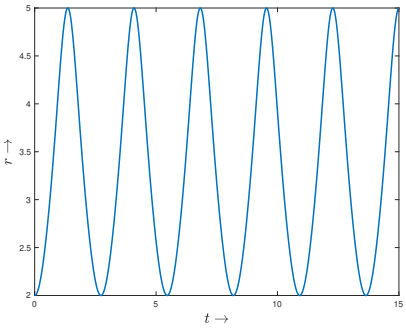

(b) $r \sim t$

Fig. 3: Case 1

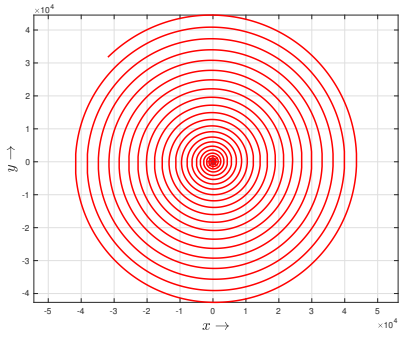

(a) Agent trajectory

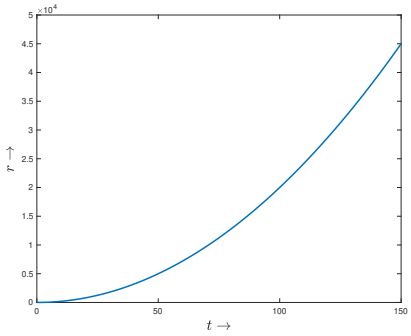

(b) $r \sim t$

Fig. 4: Case 2

These design approaches can be used to shape the trajectory beyond the boundedness criterion depending on the application of interest. In the next section, we present some simulations to elucidate these results.

IV. Simulation Results

This section represents the numerical simulations to illustrate the theoretical results obtained so far. In all of the cases, the autonomous agent is assumed to have unicycle kinematics (1). The control inputs applied to the agent are in the form of linear and angular speeds as given in (2). Without any loss of generality, the target T is assumed to be at the origin. All the parameters used in this section are in standard units.

- *Case 1:* In this case, we consider the control inputs applied to the agent as: $v(r) = r$ and $u(r) = 2r - 6$. We choose $r_0 = 2$, then (8) gives $\phi_0 = 3\pi/2$. Then, by definition, $f(r) = r^2 - 6r$ and K is calculated using (6) and initial conditions as -6. Hence, $g(r) = r^2 - 6r + 10$. The generating function is plotted as $g_2(r)$ in Fig. 2.
  The generating function has $r_{en} = 2$ and $r_{ex} = 5$ with no other extrema in $(2, 5)$. Moreover, $v(r) \neq 0$ for any r in $[2, 5]$. Thus, according to Theorem 6, the trajectory of the agent should be bounded and periodic. This is validated through Fig. 3a. It can be seen in Fig. 3b that r is bounded in $[r_{en}, r_{ex}] = [2, 5]$.
- *Case 2:* In this case, we consider the control inputs applied to the agent as: $v(r) = r$ and $u(r) = 1$. We choose the same initial conditions as *Case 1*. Again, by definition, $f(r) = r$ and $K = 4$ resulting in the generating function $g(r) = r^2 - 6r + 10$. The generating function is plotted as $g_5(r)$ in Fig. 2.
  The generating function has $r_{en} = 2$, with no other extrema in $(2, \infty)$. Moreover, $v(r) \neq 0$ for any r in $[2, \infty]$. Thus, according to Theorem 6, the trajectory of the agent should be unbounded as shown in Fig. 4a. The same can also be seen in the $r \sim t$ plot depicted in Fig. 4b, which shows that r increases monotonically in $[2, \infty)$.
- *Case 3:* Here, we assume that the initial conditions are such that $(x_0, y_0, \alpha_0) = (5, 0, 3\pi/2)$. This gives, $(r_0, \phi_0) = (5, \pi/2)$. The control inputs applied to the agent are: $v(r) = 0.5(r - 4)^2$ and $u(r) = -7(r-4)^2/(6r)$. So the generating function is: $g(r) = -7r/3 + 20/3$ which is plotted in Fig. 5d.
  As in the previous two cases, the values of r are bounded within the set $[r_{en}, r_{ex}] = [2, 5]$. In this case, $g(r)$ does not have any tangential points. However, it can be seen in Fig. 5c that $u(r) = v(r) = 0$ at $r = 4$ meaning that there is $\bar{r} > 0$ in $(2, 5)$ satisfying (10). We know from Lemma 3 and Theorem 6 that the trajectory of the agent converges to a point in this case. The same is evident from the trajectory plot in Fig. 5a. The $r \sim t$ plot in Fig. 5b shows that r values also converge to $\bar{r} = 4$ as expected.

V. Conclusions and Future Works

The paper considers an autonomous agent with unicycle kinematics. A point of interest is defined in the plane,

known as the target point. Then, the control inputs of the agent, linear and angular speeds, are designed as continuous functions of range, which the distance between the agent and the target. In contrast to our previous results in which v was assumed to be constant [17], this framework reveals a a wider class of trajectories. They can be broadly classified as bounded (and static or circular or periodic) or unbounded. The distinguishing case is when the trajectory is reaches some $\bar{r} > 0$ where $v(\bar{r}) = u(\bar{r}) = 0$. In this case, we show that the r converges to $\bar{r}$ and the trajectory converges to a single point. Keeping applications in mind, we also present a methodology to design trajectories of desired bounds and shapes. These trajectories can serve applications like surveillance of a target point, coverage, landmine de-mining, *etc*. In future, the behaviour of the agent can be studied in the presence of bearing information, instead of range.

REFERENCES

[1] A. Ratnoo, S. Y. Hayoun, A. Granot, and T. Shima, "Path following using trajectory shaping guidance," *Journal of Guidance, Control, and Dynamics*, vol. 38, no. 1, pp. 106–116, 2015.

[2] P. Tsiotras and L. I. Reyes Castro, "The artistic geometry of consensus protocols," in *Controls and Art*. Springer, 2014, pp. 129–153.

[3] T. Tripathy and A. Sinha, "Guidance of an autonomous agent for coverage applications using range only measurement," in *AIAA Guidance, Navigation, and Control (GNC) Conference*, 2013, p. 5095.

[4] R. Livermore, R. Tsalik, and T. Shima, "Elliptic guidance," *Journal of Guidance, Control, and Dynamics*, vol. 41, no. 11, pp. 2435–2444, 2018.

[5] R. Tsalik and T. Shima, "Inscribed angle guidance," *Journal of Guidance, Control, and Dynamics*, vol. 38, no. 1, pp. 30–40, 2015.

[6] T. Tripathy, A. Humne, and A. Sinha, "Generating patterns using multiple targets," in *2016 European Control Conference (ECC)*. IEEE, 2016, pp. 879–884.

[7] A. Sinha and D. Ghose, "Generalization of linear cyclic pursuit with application to rendezvous of multiple autonomous agents," *IEEE Transactions on Automatic Control*, vol. 51, no. 11, pp. 1819–1824, 2006.

[8] I. Suzuki and M. Yamashita, "Distributed anonymous mobile robots: Formation of geometric patterns," *SIAM Journal on Computing*, vol. 28, no. 4, pp. 1347–1363, 1999.

[9] A. Sinha and D. Ghose, "Generalization of nonlinear cyclic pursuit," *Automatica*, vol. 43, no. 11, pp. 1954–1960, 2007.

[10] P. Lin and Y. Jia, "Distributed rotating formation control of multi-agent systems," *Systems & Control Letters*, vol. 59, no. 10, pp. 587–595, 2010.

[11] X. Sun and C. G. Cassandras, "Optimal dynamic formation control of multi-agent systems in constrained environments," *Automatica*, vol. 73, pp. 169–179, 2016.

[12] A. Morro, A. Sgorbissa, and R. Zaccaria, "Path following for unicycle robots with an arbitrary path curvature," *IEEE Transactions on Robotics*, vol. 27, no. 5, pp. 1016–1023, 2011.

[13] X. Xiang, L. Lapierre, C. Liu, and B. Jouvencel, "Path tracking: Combined path following and trajectory tracking for autonomous underwater vehicles," in *2011 IEEE/RSJ international conference on intelligent robots and systems*. IEEE, 2011, pp. 3558–3563.

[14] P. Tsiotras and L. I. R. Castro, "Extended multi-agent consensus protocols for the generation of geometric patterns in the plane," in *Proceedings of the 2011 American Control Conference*. IEEE, 2011, pp. 3850–3855.

[15] K. S. Galloway, E. W. Justh, and P. Krishnaprasad, "Portraits of cyclic pursuit," in *2011 50th IEEE Conference on Decision and Control and European Control Conference*. IEEE, 2011, pp. 2724–2731.

[16] J.-C. Juang, "On the formation patterns under generalized cyclic pursuit," *IEEE Transactions on Automatic Control*, vol. 58, no. 9, pp. 2401–2405, 2013.

[17] T. Tripathy and A. Sinha, "Unicycle with only range input: An array of patterns," *IEEE Transactions on Automatic Control*, vol. 63, no. 5, pp. 1300–1312, 2017.

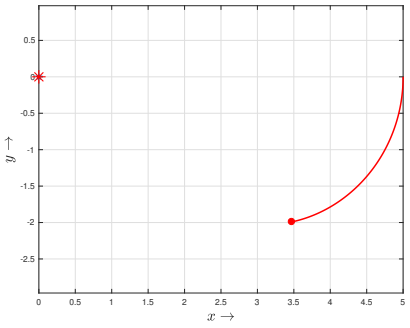

(a) Agent trajectory

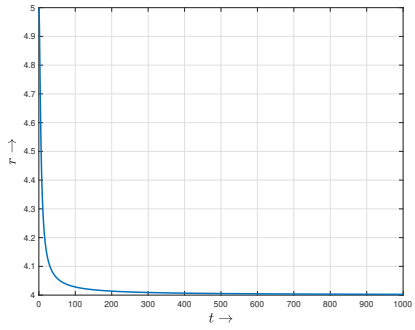

(b) $r \sim t$

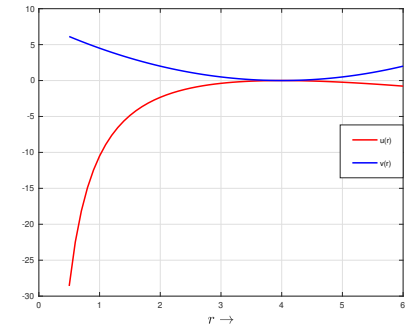

(c) $u(r),\ v(r)\ \sim r$

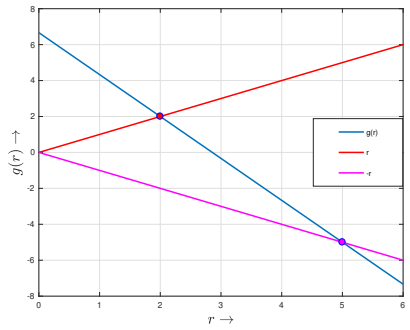

(d) $g(r) \sim t$

Fig. 5: Case 3